RESEARCH/REVIEW ARTICLE

Chemical and isotopic characteristics of a glacier-derived naled in front of Austre Grønfjordbreen, Svalbard

Jacob C. Yde[1,2,3], Andy J. Hodson[4], Irina Solovjanova[5], Jørgen P. Steffensen[6], Per Nørnberg[7], Jan Heinemeier[8] & Jesper Olsen[9]

[1] Faculty of Engineering and Science, Sogn og Fjordane University College, P.O. Box 133, NO-6851 Sogndal, Norway
[2] Department of Biological Sciences, Center for Geomicrobiology, Aarhus University, Ny Munkegade 114, DK-8000 Århus C, Denmark
[3] Bjerknes Centre for Climate Research, University of Bergen, Allégaten 55, NO-5007 Bergen, Norway
[4] Department of Geography, University of Sheffield, Sheffield S10 2TN, UK
[5] Arctic and Antarctic Research Institute, 38 Bering St., RU-199397 St. Petersburg, Russian Federation
[6] Centre for Ice and Climate, University of Copenhagen, Juliane Maries Vej 30, DK-2100 Copenhagen, Denmark
[7] Department of Earth Sciences, Aarhus University, Ny Munkegade 120, DK-8000 Århus C, Denmark
[8] Department of Physics and Astronomy, AMS ^{14}C Dating Centre, Aarhus University, Ny Munkegade 120, DK-8000 Århus C, Denmark
[9] CHRONO Centre for Climate, the Environment and Chronology, School of Geography, Archaeology and Palaeoecology, Queen's University, Belfast BT7 1NN, UK

Keywords
Naled; naled chemistry; naled isotope composition; surge-type glaciers; Svalbard.

Correspondence
Jacob C. Yde, Faculty of Engineering and Science, Sogn og Fjordane University College, P.O. Box 133, NO-6851 Sogndal, Norway.
E-mail: jacob.yde@hisf.no

Abstract

The chemical and stable isotope composition of a glacier-derived naled in front of the glacier Austre Grønfjordbreen, Svalbard, is examined to elucidate how secondary processes such as preferential retention and leaching affect naled chemistry. Internal candle ice layers have a chemical composition almost similar to that of the lower stratified granular ice layer, whereas the upper granular ice layer has a significantly different composition, which resembles the composition found in glacier meltwater. Grey, platy cryogenic calcite precipitates are found in clusters on the surface of the naled assemblage, indicating preferential retention of Ca^{2+} and HCO_3^-. This process is particular pronounced in the distal part of the naled. The isotopic composition in the naled is in accordance with the local meteoric water line and without indications of kinetic fractionation during freezing. The ability to form ice-marginal naled indicates that Austre Grønfjordbreen has the high meltwater storage potential required for triggering a glacier surge event.

Glacier naled (also termed icing or aufeis) is an extrusive ice accretion formed on proglacial outwash plains by refreezing water runoff issuing from glaciers during the cold season. Although it is widely recognized that winter runoff provides a significant contribution to the total annual solute flux from glacierized catchments (e.g., Sharp et al. 1995; Wadham et al. 2000; Yde, Knudsen & Nielsen 2005), there have been relatively few hydrochemical studies of naled. Hydrochemical data have been presented from the cold-based glacier Scott Turnerbreen (Hodgkins et al. 1997, 1998) and the surge-type polythermal glacier Finsterwalderbreen (Wadham et al. 2000), both in Svalbard. These studies have shown that naled can be considered as a solute record of highly concentrated over-winter runoff, which is released during the early ablation season. However, the solute composition can be difficult to discern due to the secondary processes of preferential retention and leaching on the naled chemistry. A common consequence of high solute content in naled is cryogenic formation of precipitates such as calcite (e.g., Lauriol et al. 1991; Bukowska-Jania 2007). At the confluence of Priestley and Corner glaciers in Antarctica, Souchez et al. (2000) found that kinetic isotope effects of δD and $\delta^{18}O$ in naled are most likely governed by differences in molecular diffusivities. This finding corresponds with data from Kuannersuit Glacier in West Greenland, where a debris-rich naled formed during a large surge event and the

Citation: *Polar Research* 2012, *31*, 17628, DOI: 10.3402/polar.v31i0.17628

subsequent glacier advance caused high proglacial stress on the naled, which resulted in thrusting and stacking of naled blocks (Yde & Knudsen 2005; Yde, Knudsen, Larsen et al. 2005). The data from Kuannersuit Glacier also indicates that the $\delta^{18}O$ isotope composition of naled is indistinguishable from other water sources such as glacial meltwater, basal ice and proglacial upwelling water (Yde & Knudsen 2005), whereas relationships between δD and deuterium excess can be used to discriminate between naled and basal ice (Yde, Knudsen, Larsen et al. 2005)

This paper aims to increase our understanding of geochemical processes in glacier naled by investigating chemical composition, stable water isotopes (δD and $\delta^{18}O$) and mineral precipitation of a naled assemblage in front of the glacier Austre Grønfjordbreen, Svalbard. Mineral precipitates on the naled surface are analysed and related to naled chemistry and freeze-concentration processes. Finally, we discuss the potential of glacier naled as an indicator for partly warm-based conditions and glacier surge activity.

Study area

Austre Grønfjordbreen (77°56′N, 14°19′E) is the eastern part of a 38 km^2 glacier complex located at the head of Grønfjorden in Nordenskiöld Land, central-west Spitsbergen, Svalbard (Fig. 1; Hagen et al. 2003). The glacier is approximately 7 km long and has a small tributary from the glacier Vestre Grønfjordbreen. The geology comprises argillites, siltstones and calcareous sandstones (Semevskij & Škatov 1965). The climate is High Arctic with a mean annual air temperature of −5.3°C (1948–2007) in the mining town of Barentsburg, situated about 13 km to the north (I. Solovjanova unpubl. data).

The Austre Grønfjordbreen naled covers an area of approximately 0.2 km^2 and has a maximum thickness of more than 1.5 m. The naled has a gentle slope of about 2° away from the glacier terminus. The naled forms in a depression, where a small outwash plain has developed as a consequence of recent glacier recession. During an 11-day period in July 2009, the naled melt rate was about 2 cm per day. Therefore, the naled is believed to have little chance to persist perennially through the ablation season, but along the margins sediment mass wasting from the lateral moraines may bury naled, in which case it may be preserved as ground ice; a process known to occur in the Canadian High Arctic (Moorman & Michel 2000). In the early ablation season, the proglacial river accelerated the melt rate of the naled near the glacier by incision or bank erosion, heat transfer and undercutting. Further downstream the river was routed into a single channel, partly controlled by obstruction by the naled.

Sampling and analytical methods

The sampling strategy comprised two objectives: (1) to excavate and sample a representative proximal naled profile and (2) to collect a set of samples from adjacent ice and water reservoirs for comparison. On 26 July 2009, the outermost 20 cm of the naled profile was carefully removed, and naled ice was collected in pre-rinsed polypropylene bottles using disposable gloves in order to avoid contamination. The samples were slowly melted at room temperature, 20 ml was decanted for isotopic analyses and the residual filtered through 0.45 μm cellulose nitrate membranes within 12 h after sampling. Mineral precipitate was collected from the surface of the naled. One sample was also collected in the outwash sediment below the naled and the pore-water was decanted into a 20 ml vial for stable isotope analyses only. On 15 July 2009, a naled ice sample was collected from the distal part of the naled assemblage (distal naled) close to the eastern lateral moraine, and a basal ice sample was collected at the glacier terminus. The sampled basal ice was classified as clean cryofacies ice according to the composite basal cryofacies terminology by Hubbard et al. (2009), as it was debris-free and only had few bubbles in crystal boundaries. Finally, a bulk glacier meltwater sample was collected at 15:30 on 26 July 2009 from the turbid proglacial river, and a lake water sample was collected on 15 July 2009 from an endorheic kettle lake (15 × 30 m in area) located within the ice-cored moraine system. The ice and water samples were collected and treated similarly to the naled profile samples. Sample storage was in darkness at about 5°C.

In the laboratory, alkalinity and pH were determined with a TitraLab TIM900 (Radiometer Analytical, Lyon, France) using 50 or 25 ml sample and 0.02 M HCl, and corrected for acidification effects during titration (ca. 31.6 $\mu mol\ l^{-1}$) following the procedure used by Yde, Knudsen & Nielsen (2005). The precision of alkalinity analyses was ±2%. In three samples (naled 2, naled 3 and naled 4) not enough meltwater was available for reliable alkalinity titrations and their HCO_3 concentrations were determined by charge balance. For the titrated samples charge balance errors (CBE) were determined as:

$$CBE = \frac{(\Sigma^+ - \Sigma^-)}{(\Sigma^+ + \Sigma^-)} \times 100\%, \quad (1)$$

where Σ^+ and Σ^- are sums of measured cation and anion equivalents, respectively. The CBEs showed slight

Citation: *Polar Research* 2012, *31*, 17628, DOI: 10.3402/polar.v31i0.17628

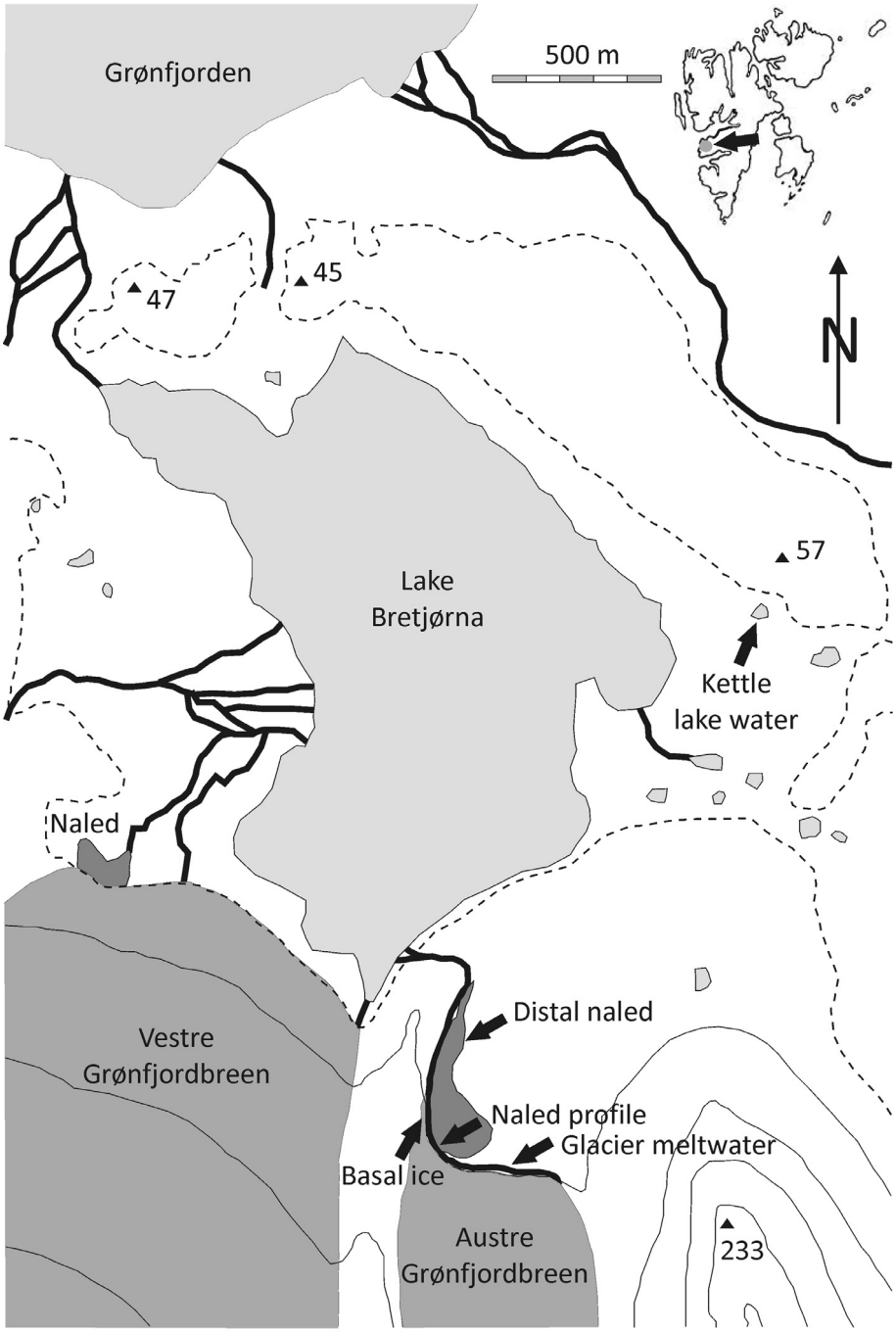

Fig. 1 Location map of Austre Grønfjordbreen, Svalbard. Naled assemblages are denoted with dark grey in front of Austre and Vestre Grønfjordbreen, and the sampling sites are marked by arrows.

excess of negative charges between −0.5 and −6.4%, which is within the total combined analytical uncertainty. Major cation (Na^+, K^+, Ca^{2+} and Mg^{2+}) and trace element (Si, Fe and Al) concentrations were measured with a 5100 PC atomic absorption spectrophotometer (Perkin–Elmer, Waltham, MA, USA). The Fe and Al concentrations were below the detection limits of 0.4 μmol l^{-1} in all samples. The analytical precision was ± 5% for Na^+ and Mg^{2+} and ± 10% for K^+, Ca^{2+} and the trace elements. Major anion (Cl^-, NO_3^- and SO_4^{2-}) concentrations were analysed on a Perkin–Elmer ion chromatograph. The NO_3^- concentration was

below the detection limit of 0.8 μmol l^{-1} in all samples, except in one (naled 4). The analytical precision of the anions was ± 5%.

Stable oxygen isotope analyses were performed at the Niels Bohr Institute, University of Copenhagen, Denmark, using mass spectrometry with a precision of ± 0.1‰ in the $\delta^{18}O$ value. Deuterium isotope analyses were performed at the AMS ^{14}C Dating Centre, University of Aarhus, Denmark, using mass spectrometry with a precision of ± 0.5‰ in the δD value.

X-ray diffraction (XRD) analyses were conducted using a D8 powder diffraction system (Bruker AXS, Madison, WI, USA) with Cu Kα radiation and a Bruker Sol-X solid-state detector.

Results

Naled stratigraphy

A naled profile was selected in a riverbank section of the proximal part of the naled, about 20 m from the glacier terminus. The naled stratigraphy is shown in Figure 2. The visual appearance and crystal texture showed that the naled was composed of five layers and two principal facies: granular ice and candle ice. The upper layer (naled 1) comprised laminated granular ice crystals with a diameter of about 1 mm and widespread occurrence of mineral precipitates. The layer had a varying thickness of 0–300 mm near the profile. Below were three distinctive anisotropic layers consisting of vertically oriented hexagonal bubble-free candle ice crystals with a length equal to the layer thickness and a horizontal diameter up to 25 mm. The thicknesses of these layers were 130 mm (naled 2), 80 mm (naled 3) and 80 mm (naled 4), respectively. The interfaces between the candle ice layers were sharp and well defined, and there were no visible accumulations of mineral precipitates along the ice crystal boundaries or at the layer interfaces. The lower layer (naled 5) had a thickness of 100 mm and showed the same physical appearance as the upper layer with horizontal laminations of varying thickness (5–50 mm) but without visible mineral precipitates. No alluvial sediments were observed to have been incorporated into the lower layer.

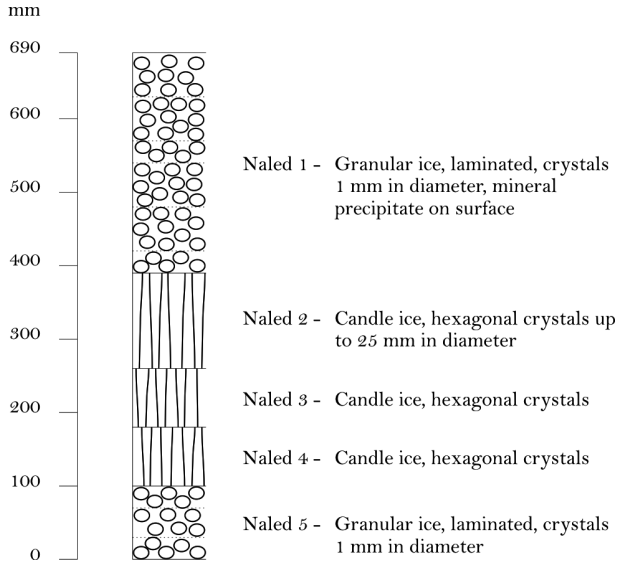

Fig. 2 Stratigraphic log of the proximal naled profile at Austre Grønfjordbreen, July 2009.

Below the naled typical glaciofluvial sediments were deposited. Lateral debris-rich ice-cored moraine ridges encircle the outwash plain and the slope of the glacier terminus is low. This suggests that the outwash sediments are, in fact, deposited on top of inactive glacier ice. A similar setting with inactive glacier ice below naled has previously been observed further north at Steenbreen (Hambrey 1984).

The naled stratigraphy with laminated snow at the top and bottom and three candle ice layers could be followed for tens of metres and should therefore be considered as representative for the upper part of the naled, although the layer thickness varied and the longest observed candle ice crystals reached a length of 180 mm.

Chemical composition

The chemical characteristics of the naled profile are shown in Table 1 together with data from other water and ice bodies in the proglacial environment of Austre Grønfjordbreen. The total dissolved solid contents ($TDS = Na^+ + K^+ + Ca^{2+} + Mg^{2+} + Si + Cl^- + NO_3^- + SO_4^{2-} + HCO_3^-$) ranged between 21 and 183 mg l^{-1}. The highest TDSs are found in basal ice, distal naled and the upper layer of the proximal naled (naled 1). Despite significant differences in geology and runoff the TDS of 77 mg l^{-1} in Austre Grønfjordbreen glacier meltwater is in good agreement with TDS in other glacial streams in Svalbard, which range between 20 mg l^{-1} at Erdmannbreen (Hodson et al. 2000) and 154 mg l^{-1} at Longyearbreen (Yde et al. 2008). The samples have neutral to slightly alkaline pH values (6.9–8.1). The partial pressures of pCO_2 are calculated as:

$$pCO_2 = \frac{(HCO_3^-)(H^+)}{K_H K_1}, \quad (2)$$

where K_H is 1021.11 mol l^{-1} atm^{-1}, K_1 is 1026.58 mol l^{-1} at 0°C and it is assumed that the ion activity coefficients are equal to 1 (Stumm & Morgan 1996).

Citation: *Polar Research* 2012, *31*, 17628, DOI: 10.3402/polar.v31i0.17628

Table 1 Chemical characteristics of naled and other water and ice bodies at Austre Grønfjordbreen, July 2009.

	pH	Na^+	K^+	Ca^{2+}	Mg^{2+}	Si	Cl^-	NO_3^-	SO_4^{2-}	HCO_3^-	TDS
	(μmol l^{-1})	(μmol l^{-1})	(μmol l^{-1})	(μmol l^{-1})	(μmol l^{-1})	(μmol l^{-1})	(μmol l^{-1})	(μmol l^{-1})	(μmol l^{-1})	(μmol l^{-1})	(mg l^{-1})
Naled 1	7.7	155	8.6	443	152	63	14	b.d.	186	1016	107
Naled 2	7.3	5.6	0.7	188	4.5	60	12	b.d.	16	347[a]	33
Naled 3	6.9	5.0	0.5	120	2.3	39	5.5	b.d.	10	224[a]	21
Naled 4	7.2	5.9	0.6	200	3.9	13	12	3.0	10	380[a]	33
Naled 5	7.5	18.7	2.1	353	17	56	15	b.d.	34	686	62
Distal naled	7.9	151	51	622	35	44	200	b.d.	52	1349	127
Glacier meltwater	7.2	78	14	325	146	17	39	b.d.	269	497	77
Basal ice	8.1	156	60	892	57	42	236	b.d.	88	1992	183
Proglacial kettle lake	7.4	94	6.0	217	65	15	125	b.d.	25	507	51

b.d. – below detection limit.
[a]HCO_3 determination by charge balance.

All samples show supersaturated pCO_2 conditions ($10^{-3.1}$–$10^{-2.8}$), indicating that proton supply exceeds chemical weathering rates.

The chemical composition in all samples is dominated by HCO_3^- and Ca^{2+} and, in the case of glacier meltwater, also by SO_4^{2-}. Although this shows that the chemical environment is primarily controlled by calcite dissolution, a detailed comparative analysis reveals more insights into the chemical variations between the samples.

The molar cation composition is shown in a ternary plot of $Na^+ + K^+$, Ca^{2+} and Mg^{2+} (Fig. 3). Proximal naled samples cluster near the Ca^{2+} corner, with the exception of naled 1 which has similar composition as glacier meltwater and kettle lake water, whereas distal naled and basal ice group together in a third cluster. This distribution indicates that in naled 2–5 calcite dissolution is by far the most significant cation source; distal naled and basal ice have inputs of $Na^+ + K^+$ from silicate weathering, evaporites or sea-spray; and naled 1, glacier meltwater and kettle lake water have a higher proportion of Mg^{2+} in addition to higher $Na^+ + K^+$.

The molar composition of HCO_3^-, $Cl^- + SO_4^{2-}$ and dissolved Si is presented in a ternary plot (Fig. 4). Most samples cluster near the HCO_3^-, but naled 2–3 have about 14% dissolved Si; naled 1 and glacier meltwater have relatively high SO_4^{2-} content (SO_4^{2-}/Cl^- ratios of 13.5 and 6.9, respectively); and distal naled, basal ice and kettle lake water have relatively high Cl^- content (SO_4^{2-}/Cl^- ratios of 0.3, 0.4 and 0.2, respectively).

In order to better assess the importance of various weathering and dissolution processes, a first-order correction of marine-derived solutes (denoted by asterisks) is obtained by multiplying the molar concentration by the ion/Cl^- ratio in seawater (e.g., Holland 1978), assuming that all Cl^- derives as atmospheric sea-spray deposition. This procedure shows an excess of Cl^- with respect to Na^+ in all samples, except naled 1, naled 5 and glacier meltwater. This Cl^- excess may be explained by preferential ion leaching of Na^+ with respect to Cl^- from the snowpack, probably enhanced by warm winter spells with positive air temperature at sea level, which are relatively common in this maritime part of Svalbard (Hanssen-Bauer et al. 1990). Austre Grønfjordbreen is located about 14.5 km from the sea and receives a significant ion contribution from deposition of sea-salts, as indicated by Cl^- concentrations of 850–1130 μmol l^{-1} in an ice core obtained at the ice divide between Vestre Grønfjordbreen and Fridtjovbreen (Vaykmyae et al. 1985) and the relatively

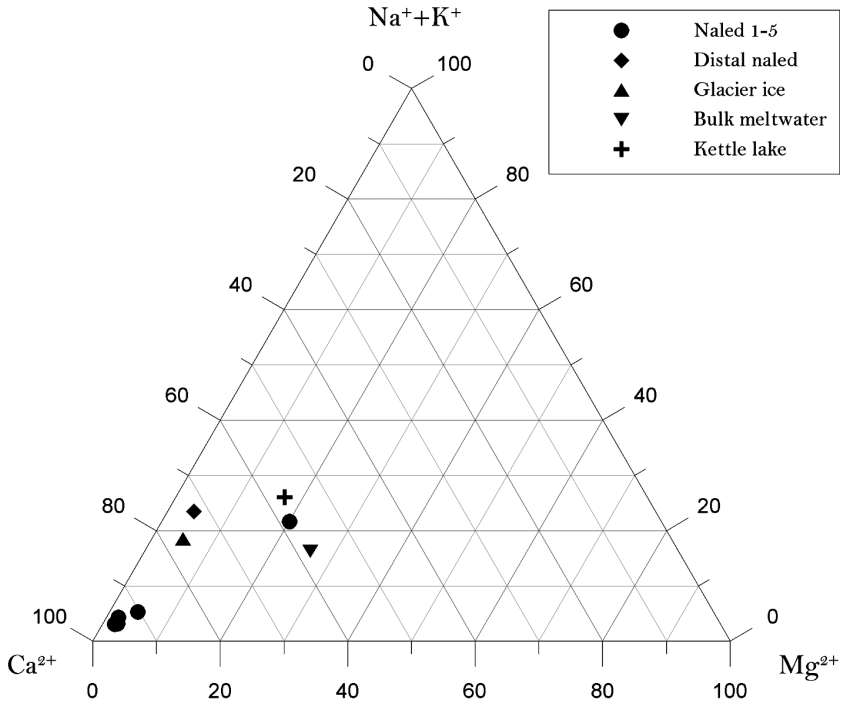

Fig. 3 Ternary plot of Mg^{2+}, $Na^{+}+K^{+}$ and Ca^{2+}.

high Cl^{-} concentration of 236 μmol l^{-1} in basal ice. Future analyses of the solute export in glacier meltwater from Austre Grønfjordbreen will provide additional insights into the proportion of marine-derived solutes.

Molar ionic ratios are generally applied to elucidate the significance of various chemical processes or solute provenances. The importance of calcite dissolution can be confirmed by $*Ca^{2+}/HCO_3^{-}$ ratios (0.42–0.65) close to

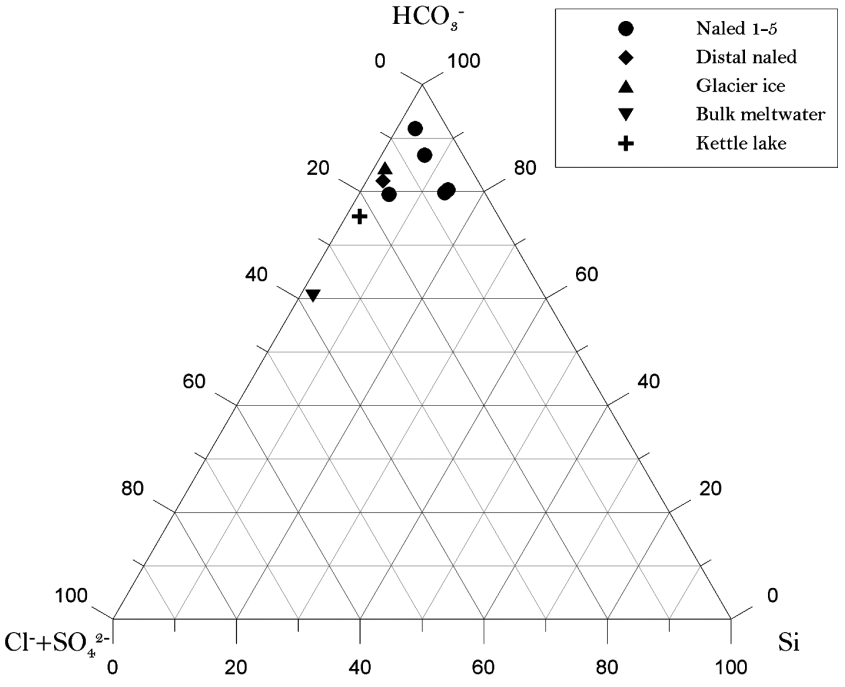

Fig. 4 Ternary plot of Si, HCO_3^{-} and $Cl^{-}+SO_4^{2-}$.

Citation: *Polar Research* 2012, *31*, 17628, DOI: 10.3402/polar.v31i0.17628

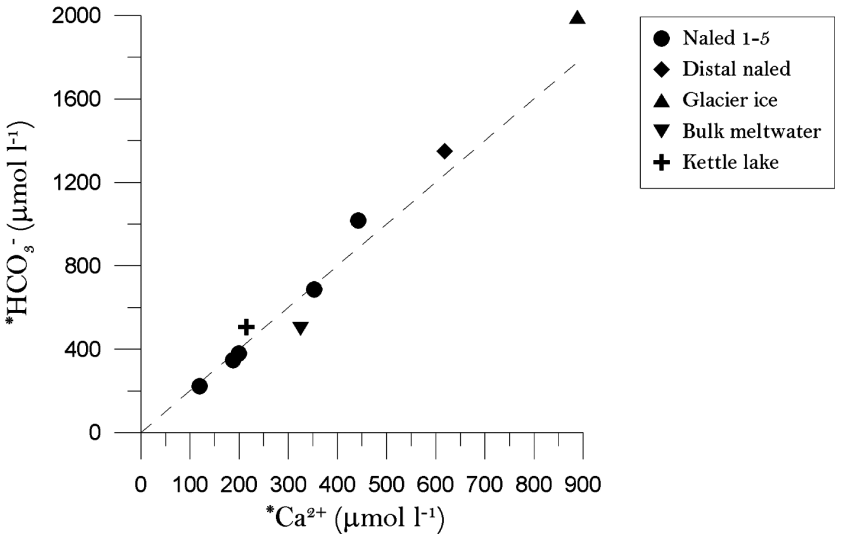

Fig. 5 Plot of $*Ca^{2+}$ versus HCO_3^-. The dashed line denotes Ca^{2+}/HCO_3^- ratio in pure calcite.

the stochiometric ratio of 0.5 for carbonation of calcite and illustrated in a $*Ca^{2+}$ versus HCO_3^- plot (Fig. 5). It is also reflected in $*Ca^{2+}/*Mg^{2+}$ ratios, which define three clusters: naled 2–4 (55–71); naled 5, distal naled and basal ice (22–39); and naled 1, glacier meltwater and kettle lake water (2.3–4.1). The relatively low $*Ca^{2+}/*Mg^{2+}$ ratios in the latter samples may indicate the occurrence of dolomite dissolution or Mg^{2+} release from silicate weathering, whereas the high $*Ca^{2+}/*Mg^{2+}$ ratios in naled 2–5 and basal ice may reflect retention of Ca^{2+} due to calcite precipitation while Mg^{2+} is leached out. The $(Ca^{2+}+Mg^{2+})/(Na^{+}+K^{+})$ ratio indicates the proportion of potential carbonate weathering (high values) to other cation provenances. The results confirm the findings from the cation ternary plot (Fig. 3), with carbonate weathering controlling the chemistry in naled 2–5 (18–31) and minor inputs from other processes contribute to the chemistry in naled 1, distal naled, basal ice, glacier meltwater and kettle lake water (2.8–5.1). However, if silicate weathering is insignificant it will be expected that the Si concentrations are low, but they are actually relatively high in naled 2–3 and naled 5, and there seems to be no correlation between Si and other potential silicate-derived ions such as Na^+ and K^+. A simple explanation may be that Na^+ and K^+ are preferentially leached out from naled, while Ca^{2+} and Si are retained.

Sulphate may derive from several sources such as sea-salts, oxidation of pyrite and dissolution of evaporites. In addition, the coal mining industry in the nearby community of Barentsburg emits substantial amounts of atmospheric acid aerosols and dust particles. The result is clearly visible on glacier surfaces in the area, where atmospheric deposition forms black carbon films (Solberg et al. 2009). High $*SO_4^{2-}$ concentrations often derive from pyrite oxidation partly coupled with carbonate dissolution, but the $*SO_4^{2-}/(*SO_4^{2-}+HCO_3^-)$ ratio in naled is less than 0.05, indicating that pyrite oxidation is relatively insignificant or that HCO_3^- is preferentially retained in naled, while SO_4^{2-} is leached out. The $*Ca^{2+}/*SO_4^{2-}$ ratio displays high values (11–22) in most samples, except in naled 1 and glacier meltwater where the $*Ca^{2+}/*SO_4^{2-}$ ratios are 2.4 and 1.2, respectively. This indicates that coupled pyrite oxidation–carbonate dissolution is important in glacier meltwater and to some extent in naled 1, while preferential retention of HCO_3^- and Ca^{2+} due to calcite precipitation is important for the chemical composition of naled. Also, notable trends are found in the correlations between $*Mg^{2+}$ and $*SO_4^{2-}$ ($R^2=0.98$) and $*Ca^{2+}$ and $*SO_4^{2-}$ ($R^2=0.96$) in all samples except naled 1, glacier meltwater and kettle lake water (Fig. 6).

Stable water isotope composition

Stable water isotope ratios ($\delta^{18}O$, δD) are often utilized to discriminate between different water sources such as snowmelt, ice-melt and liquid precipitation. Their values depend on atmospheric condensation temperature (Dansgaard 1964), mixing of input water types, and isotopic fractionation processes during phase transitions such as freezing and evaporation (Jouzel & Souchez 1982; Souchez & Jouzel 1984). At Austre Grønfjordbreen

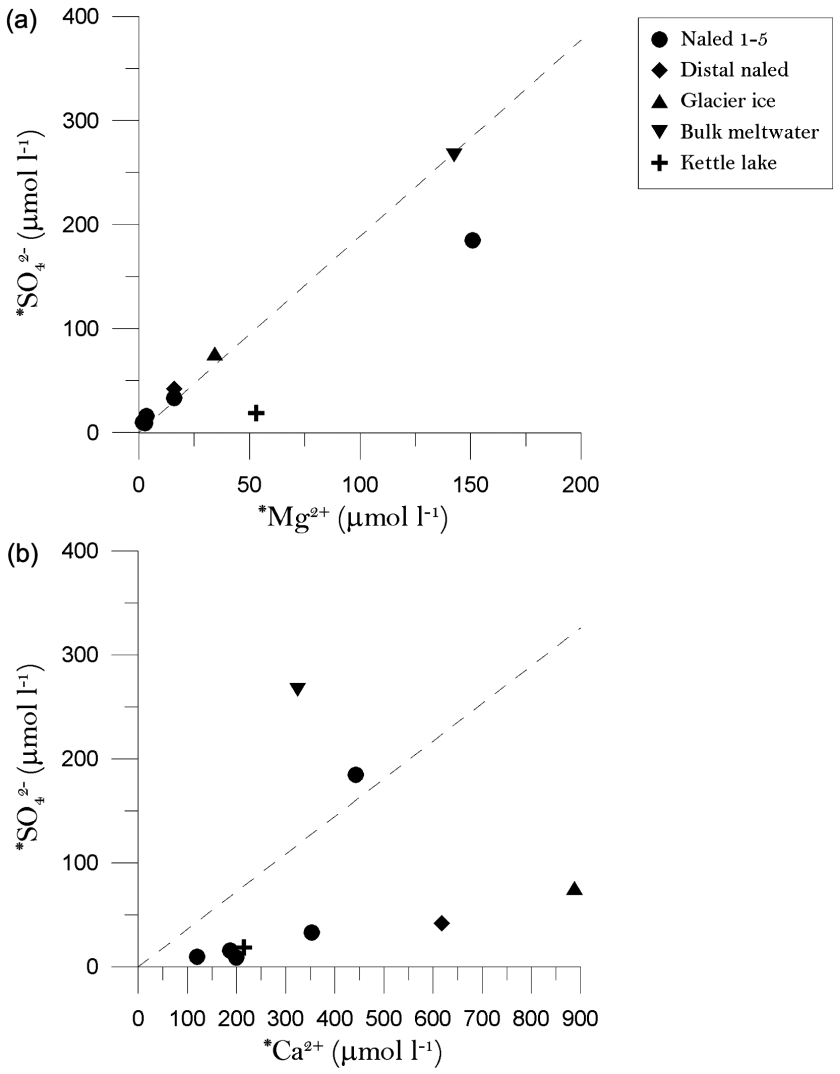

Fig. 6 Plot of (a) $*Mg^{2+}$ versus $*SO_4^{2-}$ and (b) $*Ca^{2+}$ versus $*SO_4^{2-}$. The dashed lines denote the Mg^{2+}/SO_4^{2-} and Ca^{2+}/SO_4^{2-} ratios in seawater (after Holland 1978).

the analysed $\delta^{18}O$ range between –11.7 and –9.5‰ (Table 2), which is in good agreement with the mean $\delta^{18}O$ value of –10.8‰ in the Grønfjordbreen–Fridtjovbreen ice core (Vaykmyae et al. 1985), $\delta^{18}O$ values in glacier meltwater ranging between –19.9 and –12.7‰ at Finsterwalderbreen (Wadham et al. 2004) and the mean $\delta^{18}O$ value of –13.5‰ in summer glacier meltwater at the more continental Longyearbreen, located 40 km eastwards (Yde et al. 2008). The studies at Longyearbreen also show that snowmelt has relatively low $\delta^{18}O$ values, ice-melt has intermediate $\delta^{18}O$ values and liquid precipitation has high $\delta^{18}O$ values, although considerable seasonal variations occur (Yde et al. 2008). At Austre Grønfjordbreen glacier meltwater and sub-naled sediment porewater show relatively low $\delta^{18}O$ values compared to naled 1–5, distal naled and basal ice. This indicates that glacier meltwater contains a substantial amount of snowmelt, which is very likely as the sample was collected while the snowpack was collapsing. The low $\delta^{18}O$ value in sub-naled sediment porewater suggests that the porewater primarily derives from influx of glacier meltwater into the sub-naled sediments rather than from the same water source as naled 1–5. The low $\delta^{18}O$ value in kettle lake water is expected as it is assumed that the endorheic lake is mainly fed by spring snowmelt.

The isotopic composition in naled 1–5, distal naled and basal ice is very similar, whereas glacier meltwater, sub-naled sediment porewater and kettle lake water show lighter values. A co-isotope plot is utilized to assess

Citation: *Polar Research* 2012, *31*, 17628, DOI: 10.3402/polar.v31i0.17628

Table 2 Water isotopic characteristics of naled and other water and ice bodies at Austre Grønfjordbreen, July 2009. The deuterium excess d is defined as $d = \delta^{18}O - 8\delta D$.

	$\delta^{18}O$ (‰)	δD (‰)	d (‰)
Naled 1	−9.66	−68.0	9.3
Naled 2	−9.50	−67.2	8.8
Naled 3	−9.50	−67.6	8.4
Naled 4	−10.12	−71.9	9.1
Naled 5	−9.47	−67.4	8.4
Sediment pore-water below naled	−10.89	−77.5	9.6
Distal naled	−9.84	−70.5	8.2
Glacier meltwater	−11.19	−78.5	11.0
Basal ice	−9.67	−69.4	8.0
Kettle lake water	−11.74	−85.4	8.5

whether the samples are aligned along a meteoric water line or along freezing lines with lower slopes (Fig. 7). The isotopic composition of the samples is compared with the global meteoric water line (GMWL) defined as $\delta D = 8\delta^{18}O + 10$ (Craig 1961) and the local meteoric water line (LMWL) of $\delta D = 6.46\delta^{18}O - 5.98$ ($R^2 = 0.91$; $n = 75$), which is based on composite monthly precipitation data (1961–65, 1972–75) collected at Isfjord Radio, located about 21 km to the north-west of Austre Grønfjordbreen, and provided by the International Atomic Energy Agency (IAEA/WMO 2006). With the exception of kettle lake water, all samples fit well with the LMWL which indicates that their parental waters derive from either snow or liquid precipitation without significant isotopic fractionation during freezing such as in a closed-system (Jouzel & Souchez 1982).

To determine whether evaporation or freezing are influential on the isotopic composition, the relationship between δD and deuterium excess d ($d = \delta D - 8\delta^{18}O$) is considered (Fig. 7). Evaporation and freezing cause progressive enrichment of the heavy isotopes (D, ^{18}O) in the residual water, and can be observed as a negative linear relation between deuterium excess and δD (and $\delta^{18}O$). The slope depends on prevailing conditions during evaporation or freezing such as evaporation rate, freezing rate and boundary layer thickness. This is in contrast to precipitation where correlation between δD (and $\delta^{18}O$) and deuterium excess prevails. Figure 7 shows that naled 1–5 and glacier meltwater correspond well with the LMWL ($d = \delta D - 6.46\delta^{18}O$), which signals that the proximal naled layers have developed either in a closed system or more likely in an open system with an isotopically constant parental water input that resembles the isotopic composition found in glacier meltwater or precipitation. In a previous $\delta^{18}O$ – δD study of naled in Antarctica, Souchez et al. (2000) interpreted the lack of correlation between δD and deuterium excess and the absence of an isotopic trend with naled depth as a consequence of kinetic isotope effects. Just as in Antarctica, there is no correlation between δD and deuterium excess or isotopic depth trend in the proximal naled profile at Austre Grønfjordbreen. However, this may also be due to variations in the parental water or the moisture source of precipitation events. The distal naled, basal ice and sub-naled sediment porewater exhibit a slight decrease in deuterium excess that may derive from freezing, whereas kettle lake water shows a large decrease in deuterium excess that can be explained by evaporation.

Cryogenic precipitate

The naled surface was partly covered with grey platy cryogenic precipitates (Fig. 8). XRD analysis showed that the precipitates were comprised of calcite. At places, especially on the distal part of the naled, the precipitates stood up from the surface in the form of cones up to 5 cm high, with a diameter up to 7 cm. The cones did not have an ice-core but protected the ice immediately below from melting, and most cones developed a small sun-cup depression around them. The origin of the cones is uncertain, but it is likely that calcite accumulated in cryoconite holes, which later drained leaving a pile of calcite on the surface. Sublimation and evaporation at the naled surface may further increase the calcite precipitation rate and cause local calcite supersaturation. Along the margin of the naled, calcite precipitates could be found on the ground after the naled had melted away. A significant amount of calcite was also detected in sub-naled sediments by XRD analysis, indicating that calcite saturation also is likely to occur in porewater beneath the naled. The widespread occurrence of calcite precipitate suggests that it formed in several locations where calcite saturation may occur such as in cryoconite holes, at ice-crystal boundary layers and in sediment porewater beneath the naled.

The mineral saturation state at 0°C was examined by utilizing the analytical software PHREEQC (Parkhurst & Appelo 1999). Basal ice was found to be near-saturated with respect to calcite ($SI_C = -0.04$) and slightly supersaturated with quartz ($SI_Q = 0.01$); whereas naled 1–3, naled 5 and distal naled were only supersaturated with quartz. No other minerals (e.g., gypsum) were near saturation equilibrium. The near-saturation of calcite in basal ice indicates that calcite precipitates are likely to form at the glacier sole as a consequence of melting—refreezing (regelation) processes, at least where the glacier slides over hard rock (e.g., Hallet et al. 1978). This was observed on striated hard rock in

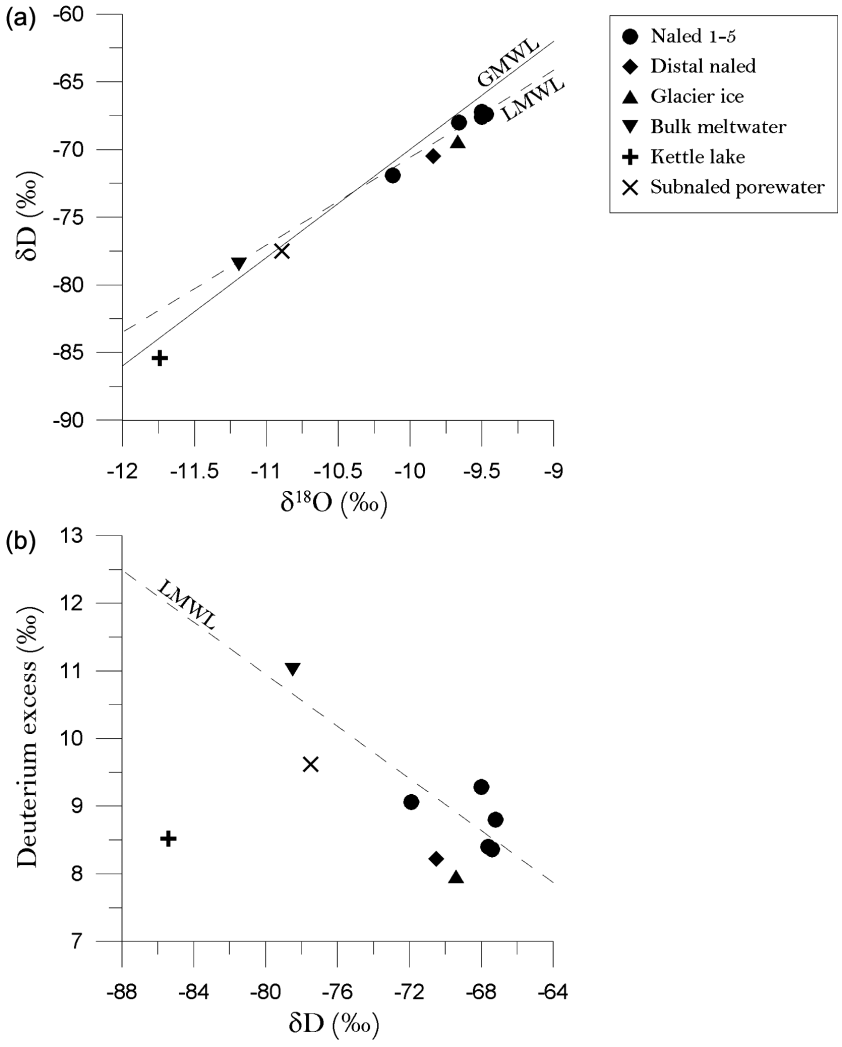

Fig. 7 (a) Co-isotope $\delta^{18}O - \delta D$ diagram. The solid line denotes the global meteoric water line (GMWL) of $\delta D = 8\delta^{18}O + 10$ (after Craig 1961) and the dashed line shows the local meteoric water line (LMWL) of $\delta D = 6.46\delta^{18}O - 5.98$ (after IAEA/WMO 2006). (b) Plot of δD versus deuterium excess *d* (defined as $d = \delta D - \delta^{18}O$). The dashed line denotes the LMWL.

front of Aldegondabreen, a glacier 6 km north of Austre Grønfjordbreen, where subglacial calcite deposits were widely distributed (Fig. 9). However, similar deposits were not observed in front of Austre Grønfjordbreen, probably because the subglacial unconsolidated sediments are well drained.

A simple PHREEQC freeze-concentration model, where pure water was gradually removed from solution in order to simulate freezing, was applied to determine when calcite saturation ($SI_C = 1$) required for formation cryogenic calcite precipitation will be reached in various solutions. The simulations show that about 77 and 88% of basal ice and distal naled, respectively, have to freeze in order to obtain calcite saturation at 0°C, whereas naled 1 and 5 have to freeze-concentrate about 94 and 96%, respectively, before calcite is saturated. In naled 2–4 and glacier meltwater the water needs to freeze-concentrate about 99% before calcite saturation is reached. These results indicate that at the time of sampling cryogenic calcite precipitation is likely to occur during freeze-up of the distal part of the naled, and subsequently in the upper layers of the proximal part of the naled. In this context it must be noted that the initial ion concentrations during naled formation differed from the ion concentrations at the time of sampling, which have been affected by secondary processes. Hence, it is likely that chemical conditions have been even more favourable for calcite precipitation during the winter season, where the naled assemblage formed.

Citation: *Polar Research* 2012, *31*, 17628, DOI: 10.3402/polar.v31i0.17628

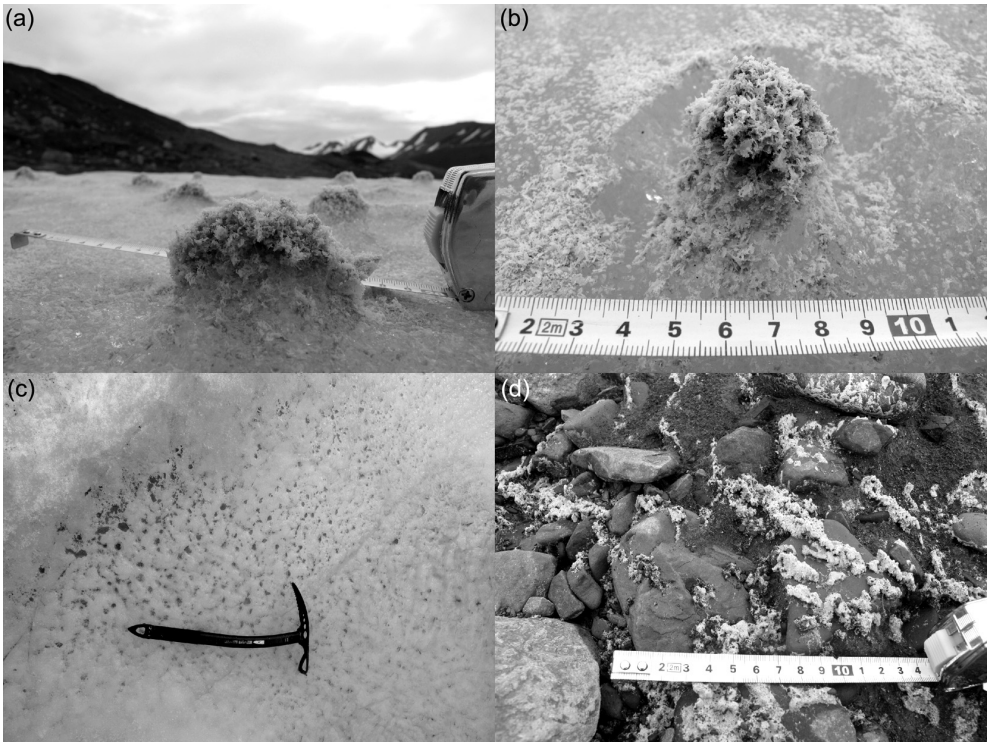

Fig. 8 (a) Picture of raised calcite precipitate cones on the naled surface; (b) oblique picture of a calcite precipitate cone showing the surrounding sun-cup and the widespread distribution of calcite precipitates on the naled surface; (c) calcite precipitate accumulation in cryoconite holes in the naled surface and (d) calcite precipitates on top of outwash sediments on a river bar after the naled has melted.

Discussion

Chemical composition of naled

The results show significant variations in the chemical and isotopic composition within the proximal naled and in comparison to adjacent water and ice reservoirs. The analyses and interpretations suggest that preferential retention of Ca^{2+} and HCO_3^- due to cryogenic calcite precipitation and preferential leaching of major ions are very important for naled chemistry. The internal candle ice layers naled 2–4 have similar chemical composition dominated by meteoric water with Ca^{2+} and HCO_3^- from carbonate weathering. The water source for naled 4 is slightly different from naled 2–3, as it has a relatively low dissolved Si content and a lower $\delta^{18}O - \delta D$ relationship with indications of some fractionation. The basal layer naled 5 has higher solute content and granular ice crystallography but otherwise resembles the candle ice layers above. In contrast, the granular top layer naled 1 is chemically different from the lower layers despite that the isotopic composition indicates that they derived from the same water source. The relatively high solute content is likely to be an artefact from the parental water, indicating that distal solute transport has been limited in the top layer. In addition, freeze-concentration caused calcite precipitation and thus removed Ca^{2+} and HCO_3^- from the initial solution. The naled 1 mutual ratios of K^+, Mg^{2+} and SO_4^{2-} are similar to what is observed in glacier meltwater, indicating that if upwelling water with a chemical composition similar to that of glacier

Fig. 9 Calcite precipitates on striated hard rock in front of Aldegondabreen, 6 km north of Austre Grønfjordbreen. The precipitation occurred in subglacial cavities as a consequence of subglacial regelation and calcite saturation.

meltwater is the parental water source for naled 1, then preferential leaching of these ions is very similar as indicated by the $*Mg^{2+}/*SO_4^{2-}$ relationship (Fig. 6).

The water source for naled is most likely proglacial upwelling water with meteoric isotope composition. This is supported by field observations of the naled apex, which is located along the glacier terminus rather than at the main glacier meltwater portal. This is similar to observations of naled in front of the adjacent glaciers Vestre Grønfjordbreen and Finsterwalderbreen (Wadham et al. 2000). The chemical composition of the water source will most likely be relatively similar to glacier meltwater, but with higher solute concentrations as observed in end-of-ablation-season meltwater (Yde et al. 2008) and a higher ratio of ions derived from chemical weathering at the expense of ions derived from marine deposition. This is due to a longer residual time for solid-solution interaction at the ice–bed interface and a lower proportion of ions leached from the snowpack.

The distal naled has higher solute concentrations and differs in ion composition from the proximal naled layers and glacier meltwater. It is enriched in Cl^- in particular, but has also increased concentrations of K^+, Ca^{2+} and HCO_3^-. This is in good correspondence with the observations of more calcite precipitate in the distal part of the naled, and the modelled lower degree of freezing in distal naled before calcite saturation is obtained. These results also support the findings by Wadham et al. (2000) that solute concentration in naled increases with distance from the water source and that preferential leaching alters the ion ratios. A chronological scenario will be that (1) parental upwelling water reaches the naled surface near the glacier terminus and is exposed to freezing; (2) as a consequence of cryogenic freeze-concentration the residual water is saturated with respect to calcite and quartz, and preferential leaching occurs and (3) subsequently the residual water is transported towards the distal part of the naled assemblage while the solute concentration increases proportional with progressive preferential leaching. The apparent relationship between ice crystallography and chemical composition may reflect the controlling parameters (i.e., water flow rate, water pressure and freezing rate) during genesis of naled layers, but detailed laboratory studies are required to further elucidate the processes involved.

Naled as indicator of basal thermal regime

The occurrence of glacier naled has in general been interpreted as a reliable indication of warm-based, or at least partly warm-based (i.e., polythermal), subglacial thermal conditions (Liestøl 1977, 1988; Åkerman 1982; Vatne et al. 1996; Glasser et al. 1999, 2004). However, it has recently become clear that glacier naled also develop in front of entirely cold-based glaciers (Hodgkins et al. 2004). A possible explanation is that meltwater may percolate from subglacial drainage channels or cavities at the bed of cold-based glaciers into permeable rocks below the glacier and flow to the proglacial zone where the meltwater emerges as up-welling water on the outwash plain. This process may be enhanced by glacier recession, exposing seasonally unfrozen sediments (Hodgkins et al. 2004) and by the bulk weight effect of glaciers on local groundwater flow potential, causing high hydraulic pressure in the proglacial zone (Åkerman 1982). Alternatively, naled in front of cold-based glaciers may derive from homothermal groundwater springs rather than from subglacial water flow. Nevertheless, the likelihood of winter runoff is significantly higher at entirely or partly warm-based glaciers than at cold-based glaciers, but the presence of glacier naled is not a diagnostic feature of warm-based conditions. There are no radio-echo sounding measurements available for Austre Grønfjordbreen, but based on the maritime location of the glacier and its size it is very likely that it is warm-based. If this is correct, then geothermal melting of basal ice may be able to sustain water supply to the subglacial drainage network throughout the winter after the initial storage of surface meltwater has depleted. This setting was found in the naled in front of the polythermal Finsterwalderbreen (Wadham et al. 2000). However, at Austre Grønfjordbreen the chemical and isotopic composition within the naled does not reveal the existence of two distinct end-members, although it may be camouflaged by the chemical alteration of the upper layer naled 1.

Naled as indicator of surge activity

Winter runoff and naled formation are common processes accompanying glacier surge events (Liestøl 1969; Åkerman 1982; Baranowski 1977, 1982; Yde & Knudsen 2005; Yde, Knudsen, Larsen et al. 2005). During active terrestrial surging, glaciers are warm-based and continuous disturbances of the subglacial drainage network may provide high potential for englacial water storage (Lingle & Fatland 2003). Stored water may be released gradually or episodically through glacier portals during the cold season and will often be very turbid, resulting in debris-rich naled assemblages (Humphrey & Raymond 1994; Yde & Knudsen 2005). In contrast, naled associated with surging glaciers in the quiescent phase is relatively debris-poor (Yde & Knudsen 2005), indicating generic evolution by slow water flow and giving the same

Citation: *Polar Research* 2012, *31*, 17628, DOI: 10.3402/polar.v31i0.17628

appearance as naled related to non-surging glaciers. Moreover, the preferential occurrence of glacier naled in front of surging glaciers may also be related to the fact that large glaciers are more likely to surge than small glaciers (Jiskoot et al. 2000; Copland et al. 2003; Jiskoot et al. 2003; Barrand & Murray 2006; Grant et al. 2009; Yde & Knudsen 2007, 2009) or that recession rates of surge-type glaciers are significantly higher than recession rates of non-surging glaciers (Yde & Knudsen 2007). In Svalbard, a survey by Bukowska-Jania & Szafraniec (2005) identified naled fields in front of 217 glaciers. Many of these are well-known surge-type glaciers (e.g., Finsterwalderbreen, Hessbreen and Werenskioldbreen) or glaciers with surge diagnostic proglacial landsystems (e.g., Elisebreen). Other glaciers have changed from a surge-type to a non-surge-type state (e.g., Midre Lovénbreen and Scott Turnerbreen) as a response to climate-forced decrease in area, volume and thickness below a surge build-up threshold, but they still form naled assemblages as long as meltwater infiltrates their subglacial drainage network. Together with other surge features, glacier naled indicates potential surge activity, but it cannot stand alone as a distinctive surge diagnostic signature.

Austre Grønfjordbreen has previously been defined as a surge-type glacier based on its prominent push moraine complex (Croot 1988), but otherwise it does not show any distinctive surge diagnostics and there are no historic observations of surge events. It is therefore generally not considered as a surge-type glacier. However, it is situated within an area with active surging glaciers and its accumulation area is adjacent to the accumulation area of Fridtjovbreen, which recently experienced a surge event with formation of push moraines (Glasser et al. 1998). The existence of naled indicates that the meltwater storage potential of Austre Grønfjordbreen is relatively high as required for triggering a surge event (e.g., Eisen et al. 2001). However, neither prominent push moraines nor glacier naled are unequivocal signs of past or present surge activity, so more evidence in the form of distinctive surge features is needed to conclude whether Austre Grønfjordbreen is in fact a surge-type glacier.

Conclusions

This paper has presented new knowledge on the chemical and stable isotope composition in glacier naled, and the findings have been related to adjacent water and ice bodies. The results show that spatial variations are reflected in the chemical composition of naled assemblages. In a proximal vertical profile the internal layers have very similar composition as the basal layer, despite differences in ice crystallography, whereas the composition of the upper layer is in many ways similar to glacier meltwater. Grey, platy cryogenic calcite precipitates are common on the naled surface, and freeze-concentration simulations indicate that calcite precipitation is particular likely to occur in the distal part of the naled assemblage. Co-isotopic analyses of $\delta^{18}O$ and δD show that naled has a composition that follows the local meteoric water line, and thus show no signs of kinetic freezing fractionation.

The naled at Austre Grønfjordbreen most likely forms by proglacial upwelling along the glacier terminus, and in this case it is a good indicator of at least partly warm-based thermal conditions and ability to store meltwater during the winter season. Although the presence of naled may be an indicator for potential glacier surging, more evidence in the form of distinctive surge features is needed to conclude whether Austre Grønfjordbreen is, in fact, a surge-type glacier.

Acknowledgements

This study is part of the Sheffield University Grønfjord Expedition funded by the University of Sheffield. JCY was funded by the Carlsberg Foundation (2007/01/0383), and AJH was funded by a Leverhulme Trust research fellowship (RF/4/RFG/2007/0398), a Royal Geographical Society Peter Fleming award and the National Geographic Research and Exploration Committee. We thank Claire Boulter, Chris Clark, Simon Chatten, Simon Cook, Matteo Spagnolo and Darrel Swift for field assistance, Bill Nandris for boat handling, and Bente Rasmussen and Birte Eriksen for laboratory assistance. We thank three reviewers for insightful comments to a previous version of this manuscript. This is publication A365 from the Bjerknes Centre for Climate Research.

References

Åkerman J. 1982. Studies on naledi (icings) in west Spitsbergen. In H.M. French (ed.): *Proceedings of the Fourth Canadian Permafrost Conference*. Pp. 189–202. Ottawa: National Research Council of Canada.

Baranowski S. 1977. Naled type of ice in front of some Spitsbergen glaciers. *Acta Universitatis Wratislaviensis 387*, 85–89.

Baranowski S. 1982. Naled ice in front of some Spitsbergen glaciers. *Journal of Glaciology 28*, 211–214.

Barrand N.E. & Murray T. 2006. Multivariate controls on the incidence of glacier surging in the Karakoram Himalaya. *Arctic, Antarctic, and Alpine Research 38*, 489–498.

Bukowska-Jania E. 2007. The role of glacier system in migration of calcium carbonate on Svalbard. *Polish Polar Research 28*, 137–155.

Bukowska-Jania E. & Szafraniec J. 2005. Distribution and morphometric characteristics of icing fields in Svalbard. *Polar Research 24*, 41–53.

Copland L., Sharp M.J. & Dowdeswell J.A. 2003. The distribution and flow characteristics of surge-type glaciers in the Canadian High Arctic. *Annals of Glaciology 36*, 73–81.

Craig H. 1961. Isotopic variations in meteoric waters. *Science 133*, 1702–1703.

Croot D.G. 1988. Glaciotectonics and surging glaciers: a correlation based on Vestspitsbergen, Svalbard, Norway. In D.G. Croot (ed.): *Glaciotectonics: forms and processes*. Pp. 49–61. Rotterdam: Balkema.

Dansgaard W. 1964. Stable isotopes in precipitation. *Tellus 16*, 436–468.

Eisen O., Harrison W.D. & Raymond C.F. 2001. The surges of Variegated Glacier, Alaska, USA, and their connection to climate and mass balance. *Journal of Glaciology 47*, 351–358.

Glasser N.F., Huddart D. & Bennett M.R. 1998. Ice-marginal characteristics of Fridtjovbreen (Svalbard) during its recent surge. *Polar Research 17*, 93–100.

Glasser N.F., Bennett M.R. & Huddart D. 1999. Distribution of glaciofluvial sediment within and on the surface of a High Arctic valley glacier: Marthabreen, Svalbard. *Earth Surface Processes and Landforms 24*, 303–318.

Glasser N.F., Coulson S.J., Hodkinson I.D. & Webb N.R. 2004. Photographic evidence of the return period of a Svalbard surge-type glacier: a tributary of Pedersenbreen, Kongsfjord. *Journal of Glaciology 50*, 307–308.

Grant K.L., Stokes C.R. & Evans I.S. 2009. Identification and characteristics of surge-type glaciers on Novaya Zemlya, Russian Arctic. *Journal of Glaciology 55*, 960–972.

Hagen J.O., Melvold K., Pinglot F. & Dowdeswell J.A. 2003. On the net mass balance of the glaciers and ice caps in Svalbard, Norwegian Arctic. *Arctic, Antarctic, and Alpine Research 35*, 264–270.

Hallet B., Lorrain R.D. & Souchez R.A. 1978. The composition of basal ice from a glacier sliding over limestones. *Geological Society of America Bulletin 89*, 314–320.

Hambrey M.J. 1984. Sedimentary processes and buried ice phenomena in the pro-glacial areas of Spitsbergen glaciers. *Journal of Glaciology 30*, 116–119.

Hanssen-Bauer I., Solas M.K. & Steffensen E.L. 1990. *The climate of Spitsbergen. DNMI-rapport/Klima 39/40*. Oslo: Norwegian Meteorological Institute.

Hodgkins R., Tranter M. & Dowdeswell J.A. 1997. Solute provenance, transport and denudation in a High Arctic glacierised catchment. *Hydrological Processes 11*, 1813–1832.

Hodgkins R., Tranter M. & Dowdeswell J.A. 1998. The hydrochemistry of runoff from a 'cold based' glacier in the High Arctic (Scott Turnerbreen, Svalbard). *Hydrological Processes 12*, 87–103.

Hodgkins R., Tranter M. & Dowdeswell J.A. 2004. The characteristics and formation of a High-Arctic proglacial icing. *Geografiska Annaler 86A*, 265–275.

Hodson A., Tranter M. & Vatne G. 2000. Contemporary rates of chemical denudation and atmospheric CO_2 sequestration in glacier basins: an Arctic perspective. *Earth Surface Processes and Landforms 25*, 1447–1471.

Holland H.D. 1978. *The chemistry of the atmosphere and oceans*. New York: Wiley.

Hubbard B., Cook S. & Coulson H. 2009. Basal ice facies: a review and unifying approach. *Quaternary Science Reviews 28*, 1956–1969.

Humphrey N.F. & Raymond C.F. 1994. Hydrology, erosion and sediment production in a surging glacier: Variegated Glacier, Alaska, 1982–83. *Journal of Glaciology 40*, 539–552.

International Atomic Energy Agency/World Meteorological Organization (IAEA/WMO) 2006. Global network of isotopes in precipitation. The GNIP database. Accessed on the internet at http://www.iaea.org/water on 12 October 2010.

Jiskoot H., Murray T. & Boyle P. 2000. Controls on the distribution of surge-type glaciers in Svalbard. *Journal of Glaciology 46*, 412–422.

Jiskoot H., Murray T. & Luckman A. 2003. Surge potential and drainage-basin characteristics in East Greenland. *Annals of Glaciology 36*, 142–148.

Jouzel J. & Souchez R.A. 1982. Melting-refreezing at the glacier sole and the isotopic composition of the ice. *Journal of Glaciology 28*, 35–42.

Lauriol B., Mars J.C. & Clark I.D. 1991. Localisation, genèse et fonte de quelques naleds du nord du Yukon (Canada). (Distribution, genesis and melting of some naledi in northern Yukon [Canada].) *Permafrost and Periglacial Processes 2*, 225–236.

Liestøl O. 1969. Glacier surges in west Spitsbergen. *Canadian Journal of Earth Science 6*, 895–897.

Liestøl O. 1977. Pingos, springs, and permafrost in Spitsbergen. *Norsk Polarinstitutt Årbok 1975*, 7–29.

Liestøl O. 1988. The glaciers in the Kongsfjorden area, Spitsbergen. *Norsk Geografisk Tidsskrift 42*, 231–238.

Lingle C.S. & Fatland D.R. 2003. Do englacial water storage drive temperature glacier surges? *Annals of Glaciology 36*, 14–20.

Moorman B.J. & Michel F.A. 2000. The burial of ice in the proglacial environment on Bylot Island, Arctic Canada. *Permafrost and Periglacial Processes 11*, 161–175.

Parkhurst D.L. & Appelo C.A.J. 1999. *User's guide to PHREEQC (version 2)—a computer program for speciation, batch-reaction, one-dimensional transport, and inverse geochemical calculations. Water-Resources Investigations Report 99-4259*. Denver: US Geological Survey.

Semevskij D.V. & Škatov E.P. 1965. Geomorfologija Zemli Nordenšel'da (Zapadnyj Špicbergen). (Geomorphology of Nordenskiöld Land [west Spitsbergen].) In V.N. Sokolov (ed.): *Materialy po geologii Špicbergena. (The geology of Spitsbergen.)* Pp. 232–240. Leningrad: Scientific Research Institute of Arctic Geology.

Citation: *Polar Research* 2012, *31*, 17628, DOI: 10.3402/polar.v31i0.17628

Sharp M.J., Tranter M., Brown G.H. & Skidmore M. 1995. Rates of chemical denudation and CO_2 drawdown in a glacier-covered alpine catchment. *Geology 23*, 61–64.

Solberg R., Bøggild C.E., Hodson A.J., Koren H., Larsen S.Ø., Trier Ø.D. & Aamaas B. 2009. Remote sensing of black carbon in the Arctic. *Proceedings of the 33rd International Symposium on Remote Sensing of Environment: sustaining the millennium development goals, May 4–9, 2009, Stresa, Italy*. Vol. 1. Pp. 41–44. Madison, WI: Omnipress.

Souchez R.A. & Jouzel J. 1984. On the isotopic composition in δD and $\delta^{18}O$ of water and ice during freezing. *Journal of Glaciology 30*, 369–372.

Souchez R.A., Jouzel J., Lorrain R., Sleewaegen S., Stiévenard M. & Verbeke V. 2000. A kinetic isotope effect during ice formation by water freezing. *Geophysical Research Letters 27*, 1923–1926.

Stumm W. & Morgan J.J. 1996. *Aquatic chemistry*. London: Wiley-Interscience.

Vatne G., Etzelmüller B., Ødegård R.S. & Sollid J.L. 1996. Meltwater routing in a High Arctic glacier, Hannabreen, northern Svalbard. *Norsk Geografisk Tidsskrift 50*, 67–74.

Vaykmyae R.A., Martma T.A., Punning Y.-M.K. & Tyugu K.R. 1985. Variations in $\delta^{18}O$ and Cl^- in an ice core from Vestfonna Nordaustlandet. *Polar Geography and Geology 9*, 329–333.

Wadham J.L., Tranter M. & Dowdeswell J.A. 2000. Hydrochemistry of meltwaters draining a polythermal-based, High-Arctic glacier, south Svalbard: II. Winter and early spring. *Hydrological Processes 14*, 1767–1786.

Wadham J.L., Bottrell S., Tranter M. & Raiswell R. 2004. Stable isotope evidence for microbial sulphate reduction at the bed of a polythermal High Arctic glacier. *Earth and Planetary Science Letters 219*, 341–355.

Yde J.C. & Knudsen N.T. 2005. Observations of debris-rich naled associated with a major glacier surge event, Disko Island, West Greenland. *Permafrost and Periglacial Processes 16*, 319–325.

Yde J.C. & Knudsen N.T. 2007. 20th-century glacier fluctuations on Disko Island (Qeqertarsuaq), Greenland. *Annals of Glaciology 46*, 209–214.

Yde J.C. & Knudsen N.T. 2009. Surge-type glaciers on Disko Island, Greenland. In M.I. Krugger & H.P. Stern (eds.): *New permafrost and glacier research*. Pp. 283–297. New York: Nova Publishers.

Yde J.C., Knudsen N.T., Larsen N.K., Kronborg C., Nielsen O.B., Heinemeier J. & Olsen J. 2005. The presence of thrust-block naled after a major surge event: Kuannersuit Glacier, West Greenland. *Annals of Glaciology 42*, 145–150.

Yde J.C., Knudsen N.T. & Nielsen O.B. 2005. Glacier hydrochemistry, solute provenance, and chemical denudation at a surge-type glacier in Kuannersuit Kuussuat, Disko Island, West Greenland. *Journal of Hydrology 300*, 172–187.

Yde J.C., Riger-Kusk M., Christiansen H.H., Knudsen N.T. & Humlum O. 2008. Hydrochemical characteristics of bulk meltwater from an entire ablation season, Longyearbreen, Svalbard. *Journal of Glaciology 54*, 259–272.